Urotensin II-related peptide (Urp) is expressed in motoneurons in zebrafish, but is dispensable for locomotion in larva

Feng Quan, Anne-Laure Gaillard, Faredin Alejevski, Guillaume Pézeron, Hervé Tostivint

Peptides
Ms # D-21-00302
Revised version

Urotensin II-related peptide (Urp) is expressed in motoneurons in zebrafish, but is dispensable for locomotion in larva

Feng B. Quan, Anne-Laure Gaillard, Faredin Alejevski[§], Guillaume Pézeron[*], Hervé Tostivint[*]

Molecular Physiology and Adaptation (PhyMA - UMR7221), Muséum national d'Histoire naturelle, CNRS, Paris, France

[§] current address: Institut de Biologie de l'Ecole Normale Supérieure (IBENS), Ecole Normale Supérieure, CNRS, INSERM, PSL Research University, Paris, France

* Co-corresponding authors:
Hervé Tostivint: htostivi@mnhn.fr (ORCID 0000-0002-0719-0922)
Guillaume Pézeron: guillaume.pezeron@mnhn.fr (ORCID 0000-0003-1395-6397)

Keywords: Urotensin 2; URP; motoneurons; zebrafish

Abstract

The *urotensin 2* (*uts2*) gene family consists of four paralogs called *uts2*, *uts2-related peptide* (*urp*), *urp1* and *urp2*. *uts2* is known to exert a large array of biological effects, including osmoregulation, control of cardiovascular functions and regulation of endocrine activities. Lately, *urp1* and *urp2* have been shown to regulate axial straightening during embryogenesis. In contrast, much less is known about the roles of *urp*. The aim of the present study was to investigate the expression and the functions of *urp* by using the zebrafish as a model.

For this purpose, we determined the expression pattern of the *urp* gene. We found that *urp* is expressed in motoneurons of the brainstem and the spinal cord, as in tetrapods. This was confirmed with a new *Tg(urp:gfp)* fluorescent reporter line. We also generated a *urp* knockout mutant by using CRISPR/Cas9-mediated genome editing and analysed its locomotor activity in larvae. *urp* mutant did not exhibit any apparent defect of spontaneous swimming when compared to wild-type.

We also tested the idea that *urp* may represent an intermediary of *urp1* and *urp2* in their role on axial straightening. We found that the upward bending of the tail induced by the overexpression of *urp2* in 24-hpf embryos was not altered in *urp* mutants. Our results indicate that *urp* does probably not act as a relay downstream of *urp*2.

In conclusion, the present study showed that zebrafish *urp* gene is primarily expressed in motoneurons but is apparently dispensable for locomotor activity in the early larval stages.

1. Introduction

Urotensin 2 (Uts2) is a cyclic neuropeptide that was first isolated from the urophysis of the teleost fish goby *Gillichthys mirabilis* [1] and subsequently identified in most vertebrate species [2]. The primary structure of Uts2 has been strongly conserved during evolution, especially at the level of the cyclic region (CFWKYC) which is shared by all species investigated so far [3,4]. In teleosts, *uts2* mRNA mainly occurs in neurosecretory neurons located in the caudal part of the spinal cord, called Dahlgren cells, that send their axons into the urophysis [5,6]. In contrast, in mammals, which are devoid of this caudal neurosecretory system, the *uts2* gene is expressed primarily in motoneurons of the brainstem and spinal cord [7–9]. Uts2 has been shown to exert various effects both in mammals and in teleosts, including osmoregulation, control of cardiovascular functions and regulation of endocrine activities [10,11]. Biological actions of Uts2 are mediated through activation of G-protein-coupled receptors called Uts2 receptor (Uts2r, aka Utr). In mammals, there is only one Uts2r [12–15], but the occurrence of up to five *uts2r* subtype genes (*uts2r1-5*) has been demonstrated in other vertebrates. Among these subtypes, *uts2r1* is the counterpart of the mammalian *uts2r* [16–18].

It is now well established that Uts2 belongs to a family of structurally related peptides that, in addition to Uts2, includes three Uts2-related peptides (Urps) called Urp, Urp1 and Urp2 [18,19]. Synteny analysis suggested that the four genes of the *uts2* family arose through the two whole-genome duplication events, called 2R, that took place early during vertebrate evolution [18–21]. Uts2, Urp, Urp1 and Urp2 exhibit the same cyclic hexapeptide core sequence while their N- and C-terminal regions are more variable.

The *urp* gene has been initially characterized in rat [22] then in chicken [22] and frog [23]. In teleosts, *urp1* and *urp2* were first reported as two co-orthologs of *urp* [24] but this view was invalidated when it appeared that both genes represent two distinct paralogs of the *uts2* family [20]. Finally, the occurrence of the genuine *urp* was demonstrated soon after in zebrafish and medaka [21]. In tetrapods, *urp*, like *uts2,* is primarily expressed in motoneurons of the brainstem and the spinal cord [23,25–27]. In the mouse spinal cord, *urp* and *uts2* transcripts were seen to co-localize in most motoneurons [27]. The *urp1* and *urp2* genes have been initially found only in teleost species [20,24] but the occurrence of either one of the two genes has subsequently been reported outside this taxon, notably in spotted gar, elephant shark, coelacanth [18,19] and frog [28]. In zebrafish, *urp1* and *urp2* mRNAs have primarily been detected in the brainstem and the spinal cord [20,29]. In the spinal cord, *urp1* and *urp2*-

expressing cells have been demonstrated to correspond to cerebrospinal fluid-contacting neurons (CSF-cNs) [29].

Up to now, the functional properties of the three Urps have been poorly studied, in contrast to those of Uts2. In mammals, Urp is able to activate Uts2r1 with the same potency as Uts2 [22], suggesting that the two peptides have some redundant functions [10,11]. However, Uts2 and Urp have also been shown to exert distinct effects, for example on astrocyte activity [4]. Despite these data, the genuine functions of Urp are still largely unknown. In zebrafish, in a recent study based on gain- and loss-of-function experiments, Urp1 and Urp2 have been suggested to regulate axial straightening during development [30]. This action appeared to require one of the zebrafish Uts2 receptor subtypes, Uts2r3, specifically expressed in muscles [30]

The study by Zhang et al. [30] illustrated that the zebrafish is a suitable model to investigate the roles of the peptides of the Uts2 family. The aim of the present study was to focus on zebrafish Urp [21]. For this purpose, we determined the expression pattern of the *urp* gene and generated urp knockout mutant by using CRISPR/Cas9-mediated genome editing.

2. Materials and methods

2.1. Nomenclature

In mammals, the gene encoding Urp neuropeptide has been named *Uts2b* (e.g. for mouse: ENSMUSG00000056423 in Ensembl). In bony fish, the gene was named *uts2d* (ENSDARG00000098149 for zebrafish in Ensembl). To avoid confusion, we will refer to this gene as *urp* in our manuscript.

Ensembl gene ID of the Uts2 receptor genes in zebrafish are the following: *uts2r1*: ENSDARG00000009624; *uts2r2*: ENSDARG00000078481; *uts2r3*: ENSDARG00000040816; *uts2r4*: ENSDARG00000096322; *uts2r5*: ENSDARG00000096870.

2.2. Animals

Zebrafish (*Danio rerio*) were bred and maintained according to standard procedures [31]. Embryos were raised at 28.5°C in E3 embryo medium and staged according to Kimmel et al. [32]. Wild-type animals were Tubingen and TL. Transgenic line *Tg(mnx1:gfp)* was previously described [33].

All procedures were approved by the Institutional Ethics Committee Cuvier at the Muséum national d'Histoire naturelle (protocols # 68–020; APAFIS#6945). In accordance to these guidelines, all efforts were made to minimize the number of animals used and their suffering.

2.3. Real time quantitative RT-PCR.

Total RNA samples were purified from entire wild type embryos, larvae or juveniles collected at the appropriate stage, and from tissues including brain, spinal cord, eyes, skin, muscle, heart, spleen, gill, gas bladder, intestine, liver, kidney, ovary and testis dissected from adults. All samples were lysed using a TissueLyser II system (Qiagen) with RNAble solution (Eurobio). Samples were treated with DNAse I (Roche) to remove potential contamination by genomic DNA and then purified with phenol/chloroform extraction. The integrity of RNA was then assayed by electrophoresis on a 1% agarose gel. cDNA samples were obtained from 2 µg of purified total RNA using Goscript reverse transcriptase (Promega) with random primers (Promega). Finally, specific cDNAs were quantified by real-time PCR using PowerUp SYBR Green (Applied Biosytem) and a QuantStudio 6 Flex instrument (Applied Biosytem). For all RT-qPCR, *lsm12B* and *mob4* were used as housekeeping genes [34]. Primer sequences are listed in Table S1. Prior to be used in qPCR, all primers pairs were assayed on 4 serial dilutions of corresponding cDNA. Linearity of CT variation on dilutions and single peak of melting curved were verified. Relative quantities were calculated using the 2e-ΔCT formula.

2.4. In situ hybridization

To generate the *urp* probe, we used a previously described full length cDNA [21] cloned into pGEMT-easy (Promega). The *urp1* and *gfp* probes were previously described [29,35]. Sense and antisense RNA probes were synthesized with SP6 or T7 transcriptase by using Digoxigenin (Dig)- and Fluorescein (Fluo)-RNA labelling mix (Roche). *In situ* hybridization (ISH) experiments were carried out following the protocols reported in previous studies [29]. In brief, embryos and dissected adult brains and spinal cords, were fixed overnight at 4°C in 4% PFA in PBS. The hybridization step was performed overnight at 65°C. Dig-/Fluo-labelled probes were detected with anti-Dig/Fluo antibodies conjugated to alkaline phosphatase (1/4000, Roche) followed by a chromogenic reaction using a solution of BM Purple (Roche) as substrate. For fluorescent ISH, labelled probes were detected using anti-Dig/Fluo antibodies conjugated to peroxidase (1/150, Roche) and revealed by Tyramide Signal

Amplification using Tyramide-FITC (PerkinElmer) or -TAMRA (Invitrogen) as substrate. For double ISH, Fluo- and Dig-labelled probed were incubated together but revealed successively, in this order. Following staining, brains and spinal cords were included in 3% agarose and sectioned at 50 µm using a vibratome (VT1000S Leica).

2.5. Immunohistochemistry

For urp – ChAT double staining, ISH was performed before immunohistochemistry and revealed using FITC- or TAMRA-conjugated tyramide. After several washes in PBS, tissues were submitted to immunostainning as described in Bougerol et al. (2015). The primary antibodies used for IHC were goat anti-choline-acetyltransferase (ChAT; 1:100, Millipore) while the secondary antibodies were donkey anti-rabbit or anti-goat IgGs coupled to Alexa Fluor 488 and Alexa Fluor 546, respectively (1:500, Life Technologies).

To detect GFP, embryos were fixed for 2 hours at room temperature or overnight at 4°C in 4% PFA in PBS. Following several washes in PBS – 0.01% Tween 20 (PBS-Tw), embryos were blocked for 1 hour at room temperature in blocking solution (1% DMSO, 1% Triton, 1% BSA and 10% Normal Goat Serum in PBS) then incubated overnight at 4°C with primary antibody in blocking solution (rabbit anti:GFP, 1:500, Life Technologies). Samples were washed in PBS – 0.5% Triton and incubated overnight at 4°C with secondary antibody in blocking solution (Alexa 488-conjugated goat anti-rabbit, 1:500, Life Technologies). Finally, embryos were washed in PBS – 0.5% Triton and mount in 80% glycerol.

2.6. Image acquisition

For single labelling, embryos were imaged on an Olympus SZX12 stereomicroscope while brain and spinal cord sections were imaged on a Leica DM5500B microscope. For fluorescent double labelling, samples were imaged on an Olympus FV1000 confocal microscope (*urp* – gfp / ChAT double staining) or on a Zeiss Axiozoom v16 (*urp* – *urp1* double staining). Whole mount GFP stained embryos were imaged on a Zeiss Axiozoom v16. Images were then processed using ImageJ [36].

2.7. Generation of transgenic lines

Transgene constructs were generated using plasmids from the tol2kit [37] and Gateway recombination system (Life technologies). For the *urp:GFPcaax* construct, a 2.6kb genomic DNA fragment, corresponding to the sequence immediately upstream of the ATG of *urp*, was

amplified by PCR (Q5 polymerase, NEB) and cloned by BP recombination into pDONRP4-P1R to produce p5E-2.6kb-urp. The final transgene was then obtained by LR recombination with the entry plasmids p5E-2.6kbURP, pME-eGFPcaax and p3E-polyA into the pDestTol2CG2 destination vector. For the *hsp:urp2* construct, the coding sequence from *urp2* was amplified by PCR (Q5 polymerase, NEB) from cDNA and cloned into pME-MCS using BamHI - XbaI. Final transgenes were then obtained by recombination with p5E-hsp70l and p3E-polyA into the pDestTol2CG2 destination vector. For transgenesis, 2 nl of a solution with 30 ng/µl of plasmid and 25 ng/µl of tol2 transposase mRNA were injected in 1 or 2 cell-stage embryos.

2.8. CRISPR/Cas9 RNA guide design and injection

Two small guide RNA (sequences in Table S1) were designed using CRISPOR (http://crispor.tefor.net/, [38]), in order to frame the region encoding for the mature peptide, and produced *in vitro* as previously described [39]. sgRNA were individually mixed with Cas9 protein to form ribonucleoprotein complexes (160 ng/µl sgRNA and 0.8 µg/µl Cas9). Embryos at 1-2 cell-stage were injected with 2 nl of a mix of the two sgRNA-Cas9 complexes and raised to adulthood. These founders were crossed against wildtype fish to screen for their ability to transmit a deleted allele by genotyping their progeny. F1 from two identified founders were raised to establish the two different mutant lines.

For genotyping, genomic DNA was extracted from either fin clips (adult) or whole embryos in 50 mM NaOH for 15 min at 95°C. After buffer neutralisation with 1/10 volume of Tris 10 mM pH 8, the DNA solution was directly used for PCR amplification (wildtype: 731 bp, mutants 556 bp and 565 bp. Primer sequences in Table S1).

2.9. Quantification of locomotor activity

Six days old larvae from crosses between *urp*$^{-/-}$ mutant females and heterozygous males, giving 50% of *MZurp*$^{-/-}$ and 50% of *urp*$^{+/-}$, were individually placed in 48-well plates. Spontaneous swimming was captured using a Noldus Daniovision system and the distance moved per minute was measured using the Ethovision software. To increase spontaneous swimming, after a habituation period of 15 minutes, larvae were submitted to a cycle of 15 minutes of dark followed by 15 minutes of light, repeated 2 times. Following records, larvae were euthanized and genotyped.

2.10. Statistics

Quantitative data were analysed using R software [40] and the tidyverse package [41]. Plots were produced using the ggplot2 packages [42]. Values are presented as mean ± SEM or boxplot (median ± interquartile range). Welch two sample t-test and Fisher's exact test were performed as indicated in figure legends.

3. Results

3.1. The urp gene is expressed in the brainstem and the spinal cord both in embryos and adults

The distribution of zebrafish *urp* mRNA in various adult tissues was examined by RT-qPCR. Figure 1 displays the relative expression of *urp* in various tissues. The *urp* transcript was mostly detected in the spinal cord with a much lower expression in the brain. To analyse the expression of *urp* in the zebrafish nervous system, we performed ISH with a Dig-labelled probe on adult tissue sections and on whole embryos from 10 hours post fertilization (hpf) to 3 days post fertilization (dpf). In the adult brain, *urp*-expressing cells were detected in two regions of the brainstem, namely the motor nucleus of the vagal nerve and in the intermediate reticular formation (Figure 2a). In the spinal cord, *urp* mRNA-containing cells were located in two parallel rows along its full length in a ventro-lateral position (Figure 2b-d).

The expression of *urp* during development was assessed using RT-qPCR. Figure 3 shows the relative expression of *urp* in whole animals from one-cell stage to juvenile stage (28 dpf). A very low expression was detected in one-cell stage embryos suggesting maternal expression. During early embryonic development, *urp* expression remained low until mid somitogenesis (16 hpf) when it increased slightly. A peak of expression was observed at 24 hpf, at the end of somitogenesis. *urp* expression was decreased at 2 dpf and a second peak was observed at 3-4 dpf. After 4 dpf, *urp* expression gradually decreased until 28 dpf.

By ISH, the first *urp*-expressing cells were observed at 16 hpf (Figure 4a) in the anterior spinal cord. At the end of somitogenesis (24 hpf, Figure 4b-c), the *urp* transcript was distributed in two parallel rows, as in adult, both in the hindbrain and the rostral part of the spinal cord. Thereafter, *urp* staining gradually disappeared from the spinal cord and was only visible in the hindbrain at 2 dpf (Figure 4d-e).

3.2. Most cells containing urp mRNA express motoneuronal markers

In both embryos and adults, *urp*-expressing cells were primarily found in the ventro-lateral part of the spinal cord, a region that corresponds to the motoneuronal domain. To test the motoneuronal identity of these cells, their ability to express two motoneuronal markers, Mnx1 (also named Hb9), a transcription factor involved in motoneuron specification [43], and ChAT (Choline-AcetylTransferase), was analysed. The expression of *mnx1* was assayed using a *Tg(mnx1:gfp)* transgenic line [33] and ChAT expression was determined using an anti-ChAT antibody. In *Tg(mnx1:gfp)* 24-hpf embryos, due to the weak expression of *urp* in the spinal cord, double-stained *urp* - *gfp* cells could be viewed only in the hindbrain. As depicted in figure 5a-c, all *urp* mRNA containing cells appeared *gfp* positive, but conversely, only a part of the latter (about 20%) contained *urp* transcript. In the adult spinal cord (Figure 5d-g), all *urp*-expressing cells were stained by the anti-ChAT antibody, but numerous ChAT immunoreactive cells did not appear to contain the *urp* mRNA.

3.3 urp is co-expressed with urp1 in some cells of the adult hindbrain.

In a previous study [29], we have observed that the *urp1* gene is expressed in two structures of the adult hindbrain, namely the motor nucleus of the vagal nerve and the reticular formation. Because both structures appeared to also contain *urp*-expressing cells, we asked whether *urp* and *urp1* are expressed in the same cells. As depicted in figure 6, *urp* and *urp1* mRNAs co-localized in the same cells of the motor nucleus of vagal nerve. In contrast, no colocalization was seen in the reticular formation (data not shown).

3.4. A transgenic reporter line suggests that urp is expressed in all motoneuron subtypes.

Our results suggested that *urp* is expressed in motoneurons in both embryos and adults. To determine whether *urp* expression is restricted to a subtype of motoneurons, we sought to visualise axonal projections of *urp*-expressing cells with a GFP reporter transgenic line. To do so, a genomic DNA fragment corresponding to the *urp* presumptive promotor, 2.6 kb immediately upstream of *urp* start codon, was cloned and placed upstream of a membrane bound GFP (GFPcaax) in a Tol2 plasmid (see methods). Consistent with *urp* expression profile, embryos injected with this plasmid exhibited mosaic GFP expression restricted to what appeared to be motoneurons (data not shown). Thus, these animals were raised to establish the *Tg(urp:gfp)* transgenic line. We assayed GFP expression in *Tg(urp:gfp)* using both ISH and immunofluorescence staining. At 1 dpf, GFP expression could not be detected.

At 2 dpf, *gfp* mRNA was detected in two rows of cells in the anterior half of the spinal cord (Figure 7a, a') and the GFP protein pattern was quite similar (Figure 7b, b').

In 3-dpf embryos, *gfp* mRNA could not be detected, however, likely due to protein stability and accumulation, GFP immunofluorescence staining was detected all along the spinal cord. GFP positive cells were organised along two rows with projections towards ventral, medial and dorsal part of each somite (Figure 7c, c', c''), suggesting GFP expression in all three subtypes of primary motoneurons (RoP, CaP, MiP) [44,45]. Besides, a large number of cells was observed in each somite, suggesting that not only primary but also secondary motoneurons expressed GFP. Overall, this profile suggested that the *Tg(urp:gfp)* line globally recapitulates the endogenous *urp* expression pattern and that Urp neuropeptide is specifically expressed in motoneurons in the spinal cord.

3.5. urp is not required for correct development and locomotion.

To investigate the function of Urp, we used CRISPR/Cas9-mediated genome edition to produce an *urp* knockout mutant line. Since the function of *urp* is likely to reside within its last exon, the one encoding for the mature peptide, we aimed at deleting this entire region. We designed two sgRNA, one on each side of the target region (Figure 8a), that were injected simultaneously into 1- or 2-cell stage embryos. We recovered two alleles, which differed for only a few nucleotides, corresponding to a complete deletion of the targeted region and thus most likely to be null (Figure 8a). We then produced homozygous $urp^{-/-}$ mutants but no abnormal phenotype was observed at morphological or global behaviour levels at any stage. Adult $urp^{-/-}$ mutant fish appeared normally viable and fertile. To test for a putative compensation effect from maternal mRNA contribution, we produced maternal and zygotic (MZ) mutants from homozygous mutant females but again these animals developed normally. Since, *urp* appeared expressed in motoneurons, we reasoned that the loss of *urp* could result in alterations of locomotor ability. To test for this possibility, we analysed spontaneous swimming of 6-dpf larvae using an automated tracking system. Control (heterozygous siblings) and MZ*urp* mutant larvae were submitted to two cycles of 15 min of dark and 15 min of light and the distanced moved per minute was measure for each larva. Overall, no significant difference was observed. In particular, the total distances moved during dark and light periods were not different (Figure 8b-c; cumulated distance during light on periods: 569 mm ± 349 (sd) and 581 mm ± 276 for controls and mutants respectively; light off periods: 971 mm ± 579 and 980 mm ± 489 for controls and mutants respectively).

Next, to test whether the absence of Urp could influence the expression of *uts2r* genes, we used RT-qPCR to measure their expression levels in 24-hpf embryos, when *urp* expression is the highest. While expression of *uts2r5* could not be reproducibly detected in neither control nor mutant (not shown), the levels of expression of *ust2r1, uts2r2* and *uts2r4* were not altered in *MZurp* mutants. In contrast, a slight decrease in *uts2r3* expression level was observed in MZ*urp* mutant embryos (Figure 8d, RQ = 1.01 ± 0.07 (sem) and 0.74 ± 0.06 for controls and mutants respectively).

It has been previously reported that the absence of phenotype of a null mutant can be due to genetic compensation. In particular, mutant mRNA degradation can trigger transcriptional adaptation [46]. To test if such a mechanism could explain the lack of apparent phenotype in *urp* mutants, we used RT-qPCR to measure the expression level of all genes of the *uts2* family in 24-hpf embryos. While our results clearly showed a reduction of *urp* mRNA in *MZurp-/-* mutants, likely due to mRNA decay, we could not detect any increase in the expression of the four other genes (Figure 8e).

3.6. Urp is not involved in axis straightness.

Several recent studies have reported the involvement of *urp1*, *urp2* and *uts2r3* in correct axis straightness in zebrafish [30,47,48]. In particular, the overexpression of the peptides in embryos results in an upward bending of the tail, likely due to localized muscle contraction [30,48]. The expression of *urp* in motoneurons prompted us to assay whether this peptide was required in this process. To test this hypothesis, we injected wildtype and *MZurp* mutant embryos with a transgenic construct driving *urp2* expression under a heat-inducible promoter. We then occasioned overexpression at 24 hpf with a heat-shock for 1 hr at 37°C. Consistent with what was previously seen in wildtype embryos [30,48], we found that overexpression of *urp2* provoked an upward bending of the tail. The effect was visible immediately at the end of the heat-shock treatment and lasted for several hours (Figure 9a, b. n= 33/38). Strikingly, the effect of *urp2* overexpression was also observed in *MZurp* mutants (Figure 9c, d. n= 22/26). Consistent with the absence of embryonic phenotype in *urp* mutants, these results suggest that Urp is not involved in axis straightness.

4. Discussion

The aim of the present study was to determine the expression pattern of the *urp* gene in zebrafish and to investigate its functional properties by genome editing and transgenesis technologies.

We found here that *urp* is primarily expressed in motoneurons of the brainstem and the spinal cord, both in embryos and adults. In support of this view, *urp-expressing* cells were shown to contain ChAT and to express *gfp* in the *Tg(mnx1:gfp)* fish transgenic line. Expression of *urp* in motoneurons has been previously reported in several species including mouse [26], chicken (HT, unpublished observations) and frog [25]. Our results thus suggest that *urp* expression in motoneurons appeared early during vertebrate evolution, before the fish-tetrapod split.

Our study revealed that *urp* expression could be detected by ISH in only a fraction of the motoneurons both in adults and in embryos. This could mean that *urp* is only expressed in a subpopulation of motoneurons. Yet, our transgenic reporter line *Tg(urp:gfp)* suggests otherwise. In this line, *gfp* mRNA expression was also found restricted to a few cells in the anterior half of the spinal cord, very much like *urp*. Nevertheless, in 3-dpf embryos immunofluorescence staining revealed GFP expression all along the spinal cord, in three types of projections (towards ventral, medial and dorsal part of each somites), and a large number of cells in each segment suggesting expression in both primary and secondary motoneurons. Thus, this observation suggests that *urp* is actually expressed in all motoneurons, although, in most cells, at a level too low to be detected by ISH.

The conserved expression of Urp in motoneurons in vertebrates suggests an important role for this peptide in these cells. In mammals however, the functional significance of Urp in motoneurons is still a matter of speculation, mainly due to the fact that its biological actions are very difficult to distinguish from those of Uts2. Two main reasons may be given for this fact: *i)* Urp and Uts2 expression patterns widely overlap in the central nervous system [26]; in particular, the vast majority of the motoneurons express both genes [27]. *ii)* Urp and Uts2 likely act through the same receptor since mammals possess only one Uts2 receptor, namely Uts2r1 [18]. Despite these reservations, several lines of evidence support the idea that Urp and/or Uts2 may be involved in the control of the locomotor activity in mammals. Intracerebroventricular (icv) injection of Uts2 in mouse and rat induces a dose-dependent increase of ambulatory movements [49–52]. In rat, Uts2 excites mesopontine cholinergic neurons [52]. In mouse cervical spinal synaptosomes, Uts2 induces a concentration-dependent stimulation of acetylcholine release [53]. Urp and/or Uts2 could also indirectly affect the

locomotor activity since Uts2 has been proposed to play a role in motoneuron differentiation, survival, and/or programmed cell death [54].

Also in trout, icv injection of Uts2 causes a long-lasting increase in motor activity [55]. However, in fish, unlike mammals, Uts2 is not expressed in motoneurons but only in a small population of neurosecretory neurons (Dahlgren cells) located at the caudal extremity of the spinal cord [5,6,56]. Thus, in fish, Urp is apparently the only member of the Uts2 family to be expressed in motoneurons and is therefore in the better position to exert the actions on locomotion previously assigned to Uts2.

In this respect, zebrafish appears as a good model to investigate the functions of the Urp released by motoneurons. For this purpose, we generated an *urp* mutant zebrafish using the CRISPR/Cas9 system. The two alleles recovered were likely to be null since the region encoding the mature cyclic peptide was deleted in both. Besides, RT-qPCR revealed that *urp* mRNA was largely decreased in *urp* mutants, suggesting mRNA decay. Since motoneurons play a central role in muscle activity and since one Uts2 receptor, Uts2r3, was recently reported to be expressed in muscle, at least in embryos [30], we analysed the locomotor activity of *urp* mutants.

To examine the impact of the *urp* knockout on the locomotor activity, we analysed spontaneous swimming of 6–dpf larvae. However, no significant difference was observed in distance travelled during recorded time between mutants and wild-type fish. This absence of a mutant phenotype was unlikely due to transcriptional adaption since we could not detect any upregulation of the other genes of the Uts2 family. Our assay was based on an automated tracking system which is relatively easy to use and was therefore perfectly suitable for a preliminary study. However, this assay could have failed to reveal subtle locomotor defects. During the last years, powerful tools have been developed based on high frequency camera that are capable of tracking simultaneously hundreds of fish and monitoring many fine swimming kinematic parameters [57–60]. A reanalysis of our *urp* mutant by using such tools will be essential for the future. Taken together, our results do not necessarily rule out a role of Urp in the locomotor activity in zebrafish. Nevertheless, if such a role exists, it is likely either modest or redundant with that of other factors. The only thing we can assume is that these factors do not belong to the Uts2 family.

Recently, two other peptides of the Uts2 family, namely Urp1 and Urp2, where proposed to regulate body straightness in zebrafish, together with the receptor Uts2r3. Zhang et al. (2018) reported that knockdown of *urp1* and *urp2*, as well as that of *uts2r3* led to similar embryonic

phenotypes. Moreover, they showed that, in embryos, the overexpression of peptides of the Uts2 family can induce an upward bending of the tail and that these peptides act through Uts2r3 since they had no effect in a *uts2r3* null background. We previously reported that in the spinal cord, *urp1* and *urp2* are specifically expressed in CSF-cNs [29]. While these cells do not contact muscles, they are known to form synaptic contacts with some motoneurons [61]. Besides, our results revealed a reduction of *uts2r3* expression in embryos deprived of Urp, suggesting that Urp could exert some function trough Uts2r3. It was thus conceivable that Urp, being expressed in motoneurons, represented an intermediary between Urp1 and Urp2 and Uts2r3. However, our results indicated that it is not likely the case since the effect of *urp2* overexpression was not affected in the *urp* null mutant.

In conclusion, the present study showed that zebrafish *urp* gene is primarily expressed in motoneurons, as in tetrapods. However, in the face of that, *urp* is apparently not required for zebrafish locomotor activity in the early larval stages. Further investigations will be needed to test its possible role in locomotion by using more accurate tools. However, in the absence of any functional evidence for an implication of Urp in locomotion, the idea that it could be involved in totally different functions must not be ruled out.

Acknowledgements

We thank Jean-Paul Chaumeil, Philippe Durand and Céline Maurice (PhyMA MNHN) for zebrafish care; Anne De Cian and Dr Jean-Paul Concordet (String MNHN) for preparing sgRNA and providing with Cas9 protein; Mathieu Carrara (PhyMA MNHN) designing and validating qPCR oligos for *lsm12* and *mob4;* Dr Caroline Parmentier (Sorbonne Université, Paris) for help with sections; Sonya Galant (Université Paris Saclay) for help in double ISH; Prof. Patrick Charnay (IBENS, Paris) for providing us with the pBS-gfp plasmid; Dr Edor Kabashi (Institut Imagine, Paris) for sharing the *Tg(mnx1:gfp)* fish transgenic line. Dr Lydia Djenoune and the team of the "Plateforme d'Imagerie Cellulaire Pitié Salpêtrière" for help in confocal imaging. Cyril Willig and the “Centre de Microscopie de fluorescence et d’IMagerie numérique” for help with in axiozoom imaging.

Declarations

Funding

This work was supported by CNRS, MNHN (ATM “Formes possibles, formes réalisées” 2015 and ATM “blanche” 2017 to G.P. and H.T.). F.A. was the recipient of a fellowship from the Alliance Sorbonne Université (programme Emergence).

Conflicts of interest/Competing interests

The authors declare no competing interests

Availability of data and material

Not applicable – material (zebrafish lines available on request)

Code availability

Not applicable

Authors' contributions

Conceptualization: Feng B. Quan, Guillaume Pézeron, Hervé Tostivint

Formal analysis: Feng B. Quan, Guillaume Pézeron, Hervé Tostivint

Investigation: Feng B. Quan, Anne-Laure Gaillard, Faredin Alejevski, Guillaume Pézeron, Hervé Tostivint

Methodology: Feng B. Quan, Guillaume Pézeron, Hervé Tostivint

Visualization: Feng B. Quan, Guillaume Pézeron, Hervé Tostivint

Supervision: Guillaume Pézeron, Hervé Tostivint

Validation: Guillaume Pézeron, Hervé Tostivint

Funding acquisition: Guillaume Pézeron, Hervé Tostivint

Writing – original draft: Guillaume Pézeron, Hervé Tostivint

Writing - review & editing: Guillaume Pézeron, Hervé Tostivint

Ethics approval

All procedures involving animals were approved by the Institutional Ethics Committee Cuvier at the Muséum national d’Histoire naturelle (protocols # 68–020; APAFIS#6945).

Consent to participate

Not applicable

Consent for publication

Not applicable

References

[1] D. Pearson, J.E. Shively, B.R. Clark, I.I. Geschwind, M. Barkley, R.S. Nishioka, H.A. Bern, Urotensin II: a somatostatin-like peptide in the caudal neurosecretory system of fishes., Proc Natl Acad Sci U A. 77 (1980) 5021–5024. https://doi.org/10.1073/pnas.77.8.5021.

[2] J.M. Conlon, Liberation of urotensin II from the teleost urophysis: an historical overview., Peptides. 29 (2008) 651–657. https://doi.org/10.1016/j.peptides.2007.04.021.

[3] J.M. Conlon, H. Tostivint, H. Vaudry, Somatostatin- and urotensin II-related peptides: molecular diversity and evolutionary perspectives, Regul Pept. 69 (1997) 95–103.

[4] M. Jarry, M. Diallo, C. Lecointre, L. Desrues, T. Tokay, D. Chatenet, J. Leprince, O. Rossi, H. Vaudry, M.-C. Tonon, L. Prézeau, H. Castel, P. Gandolfo, The vasoactive peptides urotensin II and urotensin II-related peptide regulate astrocyte activity through common and distinct mechanisms: involvement in cell proliferation, Biochem J. 428 (2010) 113–24. https://doi.org/10.1042/BJ20090867.

[5] S. Ohsako, I. Ishida, T. Ichikawa, T. Deguchi, Cloning and sequence analysis of cDNAs encoding precursors of urotensin II-alpha and -gamma, J Neurosci. 6 (1986) 2730–5.

[6] C. Parmentier, E. Hameury, I. Lihrmann, J. Taxi, H. Hardin-Pouzet, H. Vaudry, A. Calas, H. Tostivint, Comparative distribution of the mRNAs encoding urotensin I and urotensin II in zebrafish., Peptides. 29 (2008) 820–829. https://doi.org/10.1016/j.peptides.2008.01.023.

[7] Y. Coulouarn, S. Jégou, H. Tostivint, H. Vaudry, I. Lihrmann, Cloning, sequence analysis and tissue distribution of the mouse and rat urotensin II precursors, FEBS Lett. 457 (1999) 28–32.

[8] Y. Coulouarn, I. Lihrmann, S. Jegou, Y. Anouar, H. Tostivint, J.C. Beauvillain, J.M. Conlon, H.A. Bern, H. Vaudry, Cloning of the cDNA encoding the urotensin II precursor in frog and human reveals intense expression of the urotensin II gene in motoneurons of the spinal cord, Proc Natl Acad Sci U A. 95 (1998) 15803–8.

[9] S.L. Dun, G.C. Brailoiu, J. Yang, J.K. Chang, N.J. Dun, Urotensin II-immunoreactivity in the brainstem and spinal cord of the rat, Neurosci Lett. 305 (2001) 9–12.

[10] H. Vaudry, J. Leprince, D. Chatenet, A. Fournier, D.G. Lambert, J.-C.L. Mével, E.H. Ohlstein, A. Schwertani, H. Tostivint, D. Vaudry, International Union of Basic and Clinical Pharmacology. XCII. Urotensin II, Urotensin II–Related Peptide, and their receptor: from structure to function, Pharmacol. Rev. 67 (2015) 214–258. https://doi.org/10.1124/pr.114.009480.

[11] H. Vaudry, J.-C. Do Rego, J.-C. Le Mevel, D. Chatenet, H. Tostivint, A. Fournier, M.-C. Tonon, G. Pelletier, J.M. Conlon, J. Leprince, Urotensin II, from fish to human, Ann N

Acad Sci. 1200 (2010) 53–66. https://doi.org/10.1111/j.1749-6632.2010.05514.x.

[12] R.S. Ames, H.M. Sarau, J.K. Chambers, R.N. Willette, N.V. Aiyar, A.M. Romanic, C.S. Louden, J.J. Foley, C.F. Sauermelch, R.W. Coatney, Z. Ao, J. Disa, S.D. Holmes, J.M. Stadel, J.D. Martin, W.S. Liu, G.I. Glover, S. Wilson, D.E. McNulty, C.E. Ellis, N.A. Elshourbagy, U. Shabon, J.J. Trill, D.W. Hay, E.H. Ohlstein, D.J. Bergsma, S.A. Douglas, Human urotensin-II is a potent vasoconstrictor and agonist for the orphan receptor GPR14, Nature. 401 (1999) 282–6. https://doi.org/10.1038/45809.

[13] Q. Liu, S.-S. Pong, Z. Zeng, Q. Zhang, A.D. Howard, D.L. Williams, M. Davidoff, R. Wang, C.P. Austin, T.P. McDonald, C. Bai, S.R. George, J.F. Evans, C.T. Caskey, Identification of Urotensin II as the endogenous ligand for the orphan G-protein-coupled receptor GPR14, Biochem. Biophys. Res. Commun. 266 (1999) 174–178. https://doi.org/10.1006/bbrc.1999.1796.

[14] M. Mori, T. Sugo, M. Abe, Y. Shimomura, M. Kurihara, C. Kitada, K. Kikuchi, Y. Shintani, T. Kurokawa, H. Onda, O. Nishimura, M. Fujino, Urotensin II Is the endogenous ligand of a G-Protein-Coupled Orphan Receptor, SENR (GPR14), Biochem. Biophys. Res. Commun. 265 (1999) 123–129. https://doi.org/10.1006/bbrc.1999.1640.

[15] H.P. Nothacker, Z. Wang, A.M. McNeill, Y. Saito, S. Merten, B. O'Dowd, S.P. Duckles, O. Civelli, Identification of the natural ligand of an orphan G-protein-coupled receptor involved in the regulation of vasoconstriction, Nat Cell Biol. 1 (1999) 383–5. https://doi.org/10.1038/14081.

[16] L. Cui, C. Lv, J. Zhang, J. Li, Y. Wang, Characterization of four urotensin II receptors (UTS2Rs) in chickens, Peptides. 138 (2021) 170482. https://doi.org/10.1016/j.peptides.2020.170482.

[17] N. Konno, M. Takano, K. Miura, M. Miyazato, T. Nakamachi, K. Matsuda, H. Kaiya, Identification and signaling characterization of four urotensin II receptor subtypes in the western clawed frog, Xenopus tropicalis, Gen. Comp. Endocrinol. 299 (2020) 113586. https://doi.org/10.1016/j.ygcen.2020.113586.

[18] H. Tostivint, D. Ocampo Daza, C.A. Bergqvist, F.B. Quan, M. Bougerol, I. Lihrmann, D. Larhammar, Molecular evolution of GPCRS: somatostatin/urotensin II receptors, J. Mol. Endocrinol. 52 (2014) T61–T86. https://doi.org/10.1530/JME-13-0274.

[19] H. Tostivint, F.B. Quan, M. Bougerol, N.B. Kenigfest, I. Lihrmann, Impact of gene/genome duplications on the evolution of the urotensin II and somatostatin families, Gen Comp Endocrinol. 188 (2013) 110–7. https://doi.org/10.1016/j.ygcen.2012.12.015.

[20] C. Parmentier, E. Hameury, C. Dubessy, F.B. Quan, D. Habert, A. Calas, H. Vaudry, I. Lihrmann, H. Tostivint, Occurrence of two distinct urotensin II-related peptides in zebrafish provides new insight into the evolutionary history of the urotensin II gene family, Endocrinology. 152 (2011) 2330–41. https://doi.org/10.1210/en.2010-1500.

[21] F.B. Quan, M. Bougerol, F. Rigour, N.B. Kenigfest, H. Tostivint, Characterization of the true ortholog of the urotensin II-related peptide (URP) gene in teleosts, Gen Comp Endocrinol. 177 (2012) 205–12. https://doi.org/10.1016/j.ygcen.2012.02.018.

[22] T. Sugo, Y. Murakami, Y. Shimomura, M. Harada, M. Abe, Y. Ishibashi, C. Kitada, N. Miyajima, N. Suzuki, M. Mori, M. Fujino, Identification of urotensin II-related peptide as the urotensin II-immunoreactive molecule in the rat brain, Biochem Biophys Res Commun. 310 (2003) 860–8. https://doi.org/10.1016/j.bbrc.2003.09.102.

[23] N. Konno, Y. Fujii, H. Imae, H. Kaiya, T. Mukuda, M. Miyazato, K. Matsuda, M. Uchiyama, Urotensin II receptor (UTR) exists in hyaline chondrocytes: a study of peripheral distribution of UTR in the African clawed frog, Xenopus laevis, Gen Comp Endocrinol. 185 (2013) 44–56. https://doi.org/10.1016/j.ygcen.2013.01.015.

[24] S. Nobata, J.A. Donald, R.J. Balment, Y. Takei, Potent cardiovascular effects of homologous urotensin II (UII)-related peptide and UII in unanesthetized eels after peripheral and central injections, Am J Physiol Regul Integr Comp Physiol. 300 (2011) R437-46. https://doi.org/10.1152/ajpregu.00629.2010.

[25] M. Bougerol, F. Auradé, F.M. Lambert, D. Le Ray, D. Combes, M. Thoby-Brisson, F. Relaix, N. Pollet, H. Tostivint, Generation of BAC transgenic tadpoles enabling live imaging of motoneurons by using the Urotensin II-related peptide (ust2b) gene as a driver, PLoS One. 10 (2015) e0117370. https://doi.org/10.1371/journal.pone.0117370.

[26] C. Dubessy, D. Cartier, B. Lectez, C. Bucharles, N. Chartrel, M. Montero-Hadjadje, P. Bizet, D. Chatenet, H. Tostivint, E. Scalbert, J. Leprince, H. Vaudry, S. Jégou, I. Lihrmann, Characterization of urotensin II, distribution of urotensin II, urotensin II-related peptide and UT receptor mRNAs in mouse: evidence of urotensin II at the neuromuscular junction, J. Neurochem. 107 (2008) 361–374. https://doi.org/10.1111/j.1471-4159.2008.05624.x.

[27] G. Pelletier, I. Lihrmann, C. Dubessy, V. Luu-The, H. Vaudry, F. Labrie, Androgenic down-regulation of urotensin II precursor, urotensin II-related peptide precursor and androgen receptor mRNA in the mouse spinal cord, Neuroscience. 132 (2005) 689–696. https://doi.org/10.1016/j.neuroscience.2004.12.045.

[28] F. Alejevski, M. Leemans, A.-L. Gaillard, D. Leistenschneider, C. De Flori, M. Bougerol, S. Le Mével, A. Herrel, J.-B. Fini, G. Pézeron, H. Tostivint, Conserved role of the urotensin II receptor 4 signaling pathway to control body straightness in a tetrapod., Open Biol. accepted for publication (n.d.).

[29] F.B. Quan, C. Dubessy, S. Galant, N.B. Kenigfest, L. Djenoune, J. Leprince, C. Wyart, I. Lihrmann, H. Tostivint, Comparative distribution and in vitro activities of the Urotensin II-Related Peptides URP1 and URP2 in zebrafish: evidence for their colocalization in spinal Cerebrospinal Fluid-Contacting Neurons, PLoS One. 10 (2015) e0119290. https://doi.org/10.1371/journal.pone.0119290.

[30] X. Zhang, S. Jia, Z. Chen, Y.L. Chong, H. Xie, D. Feng, X. Wu, D.Z. Song, S. Roy, C. Zhao, Cilia-driven cerebrospinal fluid flow directs expression of urotensin neuropeptides to straighten the vertebrate body axis, Nat. Genet. 50 (2018) 1666–1673. https://doi.org/10.1038/s41588-018-0260-3.

[31] M. Westerfield, The zebrafish book. A guide for the laboratory use of zebrafish (Danio rerio)., 4th ed., Univ. of Oregon Press, Eugene., 2000.

[32] C.B. Kimmel, W.W. Ballard, S.R. Kimmel, B. Ullmann, T.F. Schilling, Stages of embryonic development of the zebrafish, Dev Dyn. 203 (1995) 253–310. https://doi.org/10.1002/aja.1002030302.

[33] H. Flanagan-Steet, M.A. Fox, D. Meyer, J.R. Sanes, Neuromuscular synapses can form in vivo by incorporation of initially aneural postsynaptic specializations, Development. 132 (2005) 4471–4481. https://doi.org/10.1242/dev.02044.

[34] Y. Hu, S. Xie, J. Yao, Identification of novel Reference genes suitable for qRT-PCR normalization with respect to the zebrafish developmental stage, PLOS ONE. 11 (2016) e0149277. https://doi.org/10.1371/journal.pone.0149277.

[35] C. Labalette, M.A. Wassef, C. Desmarquet-Trin Dinh, Y.X. Bouchoucha, J. Le Men, P. Charnay, P. Gilardi-Hebenstreit, Molecular dissection of segment formation in the developing hindbrain, Development. 142 (2015) 185–195. https://doi.org/10.1242/dev.109652.

[36] C.A. Schneider, W.S. Rasband, K.W. Eliceiri, NIH Image to ImageJ: 25 years of image analysis, Nat. Methods. 9 (2012) 671–675. https://doi.org/10.1038/nmeth.2089.

[37] K.M. Kwan, E. Fujimoto, C. Grabher, B.D. Mangum, M.E. Hardy, D.S. Campbell, J.M. Parant, H.J. Yost, J.P. Kanki, C.-B. Chien, The Tol2kit: a multisite gateway-based construction kit for Tol2 transposon transgenesis constructs, Dev Dyn. 236 (2007) 3088–99. https://doi.org/10.1002/dvdy.21343.

[38] M. Haeussler, K. Schönig, H. Eckert, A. Eschstruth, J. Mianné, J.-B. Renaud, S. Schneider-Maunoury, A. Shkumatava, L. Teboul, J. Kent, J.-S. Joly, J.-P. Concordet, Evaluation of off-target and on-target scoring algorithms and integration into the guide RNA selection tool CRISPOR, Genome Biol. 17 (2016) 148. https://doi.org/10.1186/s13059-016-1012-2.

[39] T.O. Auer, K. Duroure, J.-P. Concordet, F. Del Bene, CRISPR/Cas9-mediated conversion of eGFP- into Gal4-transgenic lines in zebrafish, Nat Protoc. 9 (2014) 2823–40. https://doi.org/10.1038/nprot.2014.187.

[40] R Core Team, R: A Language and Environment for Statistical Computing, (2021). https://www.R-project.org/.

[41] H. Wickham, M. Averick, J. Bryan, W. Chang, L.D. McGowan, R. François, G. Grolemund, A. Hayes, L. Henry, J. Hester, M. Kuhn, T.L. Pedersen, E. Miller, S.M. Bache, K. Müller, J. Ooms, D. Robinson, D.P. Seidel, V. Spinu, K. Takahashi, D. Vaughan, C. Wilke, K. Woo, H. Yutani, Welcome to the tidyverse, J. Open Source Softw. 4 (2019) 1686.

[42] H. Wickham, ggplot2: Elegant Graphics for Data Analysis, Springer-Verlag New York, 2016. https://ggplot2.tidyverse.org.

[43] S. Arber, B. Han, M. Mendelsohn, M. Smith, T.M. Jessell, S. Sockanathan, Requirement for the homeobox gene Hb9 in the consolidation of motor neuron identity, Neuron. 23 (1999) 659–674. https://doi.org/10.1016/s0896-6273(01)80026-x.

[44] K.E. Lewis, J.S. Eisen, From cells to circuits: development of the zebrafish spinal

cord, Prog Neurobiol. 69 (2003) 419–49.

[45] P.Z. Myers, J.S. Eisen, M. Westerfield, Development and axonal outgrowth of identified motoneurons in the zebrafish, J. Neurosci. 6 (1986) 2278–2289. https://doi.org/10.1523/JNEUROSCI.06-08-02278.1986.

[46] M.A. El-Brolosy, Z. Kontarakis, A. Rossi, C. Kuenne, S. Günther, N. Fukuda, K. Kikhi, G.L.M. Boezio, C.M. Takacs, S.-L. Lai, R. Fukuda, C. Gerri, A.J. Giraldez, D.Y.R. Stainier, Genetic compensation triggered by mutant mRNA degradation, Nature. (2019). https://doi.org/10.1038/s41586-019-1064-z.

[47] Y. Cantaut-Belarif, A. Orts Del'Immagine, M. Penru, G. Pézeron, C. Wyart, P.-L. Bardet, Adrenergic activation modulates the signal from the Reissner fiber to cerebrospinal fluid-contacting neurons during development, ELife. 9 (2020) e59469. https://doi.org/10.7554/eLife.59469.

[48] H. Lu, A. Shagirova, J.L. Goggi, H.L. Yeo, S. Roy, Reissner fibre-induced urotensin signalling from cerebrospinal fluid-contacting neurons prevents scoliosis of the vertebrate spine, Biol. Open. 9 (2020). https://doi.org/10.1242/bio.052027.

[49] J. Gartlon, F. Parker, D.C. Harrison, S.A. Douglas, T.E. Ashmeade, G.J. Riley, Z.A. Hughes, S.G. Taylor, R.P. Munton, J.J. Hagan, J.A. Hunter, D.N. Jones, Central effects of urotensin-II following ICV administration in rats, Psychopharmacology (Berl.). 155 (2001) 426–433. https://doi.org/10.1007/s002130100715.

[50] J.-C. Do-Rego, D. Chatenet, M.-H. Orta, B. Naudin, C. Le Cudennec, J. Leprince, E. Scalbert, H. Vaudry, J. Costentin, Behavioral effects of urotensin-II centrally administered in mice, Psychopharmacology (Berl.). 183 (2005) 103–117. https://doi.org/10.1007/s00213-005-0140-2.

[51] J.-C. do Rego, J. Leprince, E. Scalbert, H. Vaudry, J. Costentin, Behavioral actions of urotensin-II, Peptides. 29 (2008) 838–844. https://doi.org/10.1016/j.peptides.2007.12.016.

[52] S.D. Clark, H.-P. Nothacker, C.D. Blaha, C.J. Tyler, D.M. Duangdao, S.L. Grupke, D.R. Helton, C.S. Leonard, O. Civelli, Urotensin II acts as a modulator of mesopontine cholinergic neurons, Brain Res. 1059 (2005) 139–148. https://doi.org/10.1016/j.brainres.2005.08.026.

[53] F. Bruzzone, C. Cervetto, M.C. Mazzotta, P. Bianchini, E. Ronzitti, J. Leprince, A. Diaspro, G. Maura, M. Vallarino, H. Vaudry, M. Marcoli, Urotensin II receptor and acetylcholine release from mouse cervical spinal cord nerve terminals, Neuroscience. 170 (2010) 67–77. https://doi.org/10.1016/j.neuroscience.2010.06.070.

[54] Y. Coulouarn, C. Fernex, S. Jégou, C.E. Henderson, H. Vaudry, I. Lihrmann, Specific expression of the urotensin II gene in sacral motoneurons of developing rat spinal cord, Mech. Dev. 101 (2001) 187–190. https://doi.org/10.1016/s0925-4773(00)00548-7.

[55] G. Vanegas, J. Leprince, F. Lancien, N. Mimassi, H. Vaudry, J.-C. Le Mével, Divergent cardio-ventilatory and locomotor effects of centrally and peripherally administered urotensin II and urotensin II-related peptides in trout, Front. Neurosci. 9 (2015) 142. https://doi.org/10.3389/fnins.2015.00142.

[56] W. Lu, M. Greenwood, L. Dow, J. Yuill, J. Worthington, M.J. Brierley, C.R. McCrohan, D. Riccardi, R.J. Balment, Molecular characterization and expression of Urotensin II and its receptor in the flounder (Platichthys flesus): A hormone system supporting body fluid homeostasis in euryhaline fish, Endocrinology. 147 (2006) 3692–3708. https://doi.org/10.1210/en.2005-1457.

[57] B.H. Bishop, N. Spence-Chorman, E. Gahtan, Three-dimensional motion tracking reveals a diving component to visual and auditory escape swims in zebrafish larvae, J. Exp. Biol. 219 (2016) 3981–3987. https://doi.org/10.1242/jeb.147124.

[58] R.E. Johnson, S. Linderman, T. Panier, C.L. Wee, E. Song, K.J. Herrera, A. Miller, F. Engert, Probabilistic models of larval zebrafish behavior eeveal structure on many scales, Curr. Biol. 30 (2020) 70-82.e4. https://doi.org/10.1016/j.cub.2019.11.026.

[59] O. Mirat, J.R. Sternberg, K.E. Severi, C. Wyart, ZebraZoom: an automated program for high-throughput behavioral analysis and categorization, Front. Neural Circuits. 7 (2013). https://doi.org/10.3389/fncir.2013.00107.

[60] F.B. Quan, L. Desban, O. Mirat, M. Kermarquer, J. Roussel, F. Koëth, H. Marnas, L. Djenoune, F.-X. Lejeune, H. Tostivint, C. Wyart, Somatostatin 1.1 contributes to the innate exploration of zebrafish larva, Sci. Rep. 10 (2020) 15235. https://doi.org/10.1038/s41598-020-72039-x.

[61] J.M. Hubbard, U.L. Böhm, A. Prendergast, P.-E.B. Tseng, M. Newman, C. Stokes, C. Wyart, Intraspinal sensory neurons provide powerful inhibition to motor circuits ensuring postural control during locomotion, Curr. Biol. CB. 26 (2016) 2841–2853. https://doi.org/10.1016/j.cub.2016.08.026.

[62] M.F. Wullimann, B. Rupp, H. Reichert, The brain of the zebrafish Danio rerio: a neuroanatomical atlas, in: M.F. Wullimann, B. Rupp, H. Reichert (Eds.), Neuroanat. Zebrafish Brain Topol. Atlas, Birkhäuser, Basel, 1996: pp. 19–87. https://doi.org/10.1007/978-3-0348-8979-7_5.

Figure legends

Fig. 1. Tissue distribution of *urp* mRNA in adult zebrafish assessed by RT-qPCR. Means from four to six independent experiments are presented. Error-bars are s.e.m.

Fig. 2. Expression of *urp* in adult brain and spinal cord. Localization of *urp* mRNA revealed by in ISH in the brainstem (a) and spinal cord (b-d) of adult zebrafish. (a) Transverse section of the brainstem. The anatomical structures indicated on the right hemisection are designated according to Wullimann et al. [62]. Parasagittal (b) and transverse (c) sections of the spinal cord. Ventral view of whole-mount spinal cord (d). Dig-labelled *urp* probe is revealed in violet. DV, descending trigeminal root; Flv, funiculus lateralis pars ventralis; Fv, funiculus ventralis; IRF, inferior reticular formation; LX, lobus vagus; Mauthner axon; MFN, medial funicular nucleus; MLF, medial longitudinal fascicle; NXm, motor nucleus of the vagal nerve; RV, rhombencephalic ventricle; SGT, secondary gustatory tract; TBS, tractus bulbospinalis. Scale bars: 100 μm

Fig. 3. Expression dynamics of *urp* during zebrafish development. *urp* expression levels were assayed by RT-qPCR from fertilization (0 hpf) to juvenile stage (28 dpf). Means from five or six independent experiments are presented. Error-bars are s.e.m.

Fig. 4. Expression profile of *urp* during zebrafish embryogenesis. Localization of *urp* mRNA revealed by in ISH in zebrafish embryos. During somitogenesis, *urp* is detected in two rows of cells in the anterior half of the forming spinal cord (a-c). At 24 hpf, *urp* is also detected in a small cluster of cells in the hindbrain (b). At 34 hpf, *urp* expression in the spinal cord is progressively reduced to the most anterior part of the spinal cord. The expression in the hindbrain is increased (d). From 48 hpf, *urp* is only detected in the hindbrain. a, b, d and e, lateral view; c, dorsal view. h, hindbrain; sc, spinal cord.

Fig. 5. *urp* is expressed in motoneurons both in embryos and adults. (a-c) Localization of *urp* and *gfp* mRNAs revealed by double fluorescence whole-mount ISH on *Tg(mnx1:gfp)* zebrafish embryos at 24 hpf (dorsal views). *gfp* is in green (a) and *urp* in red (b). A merge with DAPI in blue is presented in (c). Double-labelled cells are indicated by arrows. Scale bar: 15 μm. (d-f) Localization of *urp* mRNA revealed by fluorescent ISH together with a fluorescent immunostaining for ChAT on adult zebrafish spinal cord (sagittal section). ChAT

730 is in green (d) and *urp* in red (e). A merge is presented in (f). Double-labelled cells are
731 indicated by arrows. Scale bar: 100 µm.
732
733 **Fig. 6.** *urp* and *urp1* are co-expressed in some cells in the adult hindbrain. Co-localisation of
734 *urp* and *urp1* mRNAs revealed by double fluorescent ISH on adult hindbrain sections at the
735 level of the motor nucleus of vagal nerve. *urp1* is in red (a) and *urp* in green (b). A merge
736 with DAPI in blue is presented in (c). Scale bar: 100 µm.
737
738 **Fig. 7.** Expression profile of *Tg(urp:gfp).* (a, a') Localization of *gfp* mRNA revealed by ISH
739 in 2-dpf embryos. (b-c'') Localization of GFP protein revealed by immunofluorescent
740 staining in 2-dpf embryos (b, b') and 3-dpf embryos (c-c''). Note the two rows of *gfp*-
741 expressing cells in the spinal cord (blue and white arrowhead) and the three types of
742 projection (ventral, dorsal and medial, arrows in c''). GFP expression in the heart (asterisks)
743 is due to the presence of transgene marker (*clmc:gfp)* in the transgene. a, b, c and c'', lateral
744 view; a', b' and c', dorsal view. Scale bar: 100 µm.
745
746 **Fig. 8.** MZ*urp* mutant exhibit normal locomotor ability in spontaneous swimming. (a) The
747 wildtype genomic sequence of the *urp* locus, around the fifth exon encoding the core of the
748 mature peptide, is aligned with the two mutant alleles obtained in this study. The
749 corresponding wildtype peptide sequence is indicated above with the mature peptide sequence
750 highlighted in orange. On the wildtype sequence, exons are in bold, coding sequence in upper
751 case and the position of the two guide RNA is indicated in green (+ PAM in yellow). The two
752 mutant alleles correspond to a deletion of the sequence between the two guides with a small
753 insertion in the second allele (in red). A motility assay was performed on *MZurp* mutants (n =
754 51 mutants and 45 sibling controls). (b) Average distance covered per minutes during the
755 motility assay. Dark periods (i.e. light off) are indicated by grey area. (c) Cumulated distance
756 covered during light on and light off (dark) periods (30 min total per period; Welch Two
757 Sample t-test, $p = 0.80$ and $p = 0.91$ and for light on and light off (dark) periods respectively).
758 (d, e) Expression levels of genes encoding for four Uts2 receptors (d) and the five peptides of
759 the Uts2 family (e) assayed by RT-qPCR in wildtype or *MZurp* mutant 24-hpf embryos. Data
760 were collected from five independent clutches and represented as mean ± SEM. Welch two
761 sample t-test, p-value are indicated on each panel.
762

Fig. 9. *urp* is not involved in axis straightness in zebrafish embryos. (a, b) In wildtype embryos, overexpressing *urp2* resulted in upward bending of the tail (n = 33/38). (c, d) The effect of *urp2* overexpression was not altered in *MZurp* mutants (n = 22/26. Fisher's exact test, p-value = 1).

Supplementary data

Table S1. Sequences of the oligonucleotides used for PCR amplifications and genome editing

Oligoname	sequence
genotyping	
URP_genotyp_F	GACTGGAGTTGGCCAGGAAA
URP_genotyp_R	ACACTAGAGGGAGACAACAGC
Real-time PCR	
urp_qPCR_F	GCGGAAAAATGTCATGCCTCTTC
urp_qPCR_R	TTGAGCTCCTTTTGAAGCTCCTG
uts2a_qPCR_F	CACTGCTCAACAGAGACAGTATCA
uts2a_qPCR_R	CCAAAAGACCACTGGGAGGAAC
uts2b_qPCR_F	TACCCGTCTCTCATCAGTGGAG
uts2b_qPCR_R	TTTTCCAGCAAGGCCTCTTTTAC
urp1_qPCR_F	ACATTCTGGCTGTGGTTTGTTC
urp1_qPCR_R	CTCTTTTGCACCTCTCTGAAGC
urp2_qPCR_F	ACCAGAGGAAACAGCAATGGAC
urp2_qPCR_R	TGAGGTTTCCATCCGTCACTAC
uts2r1_qPCR_F	CTCCTTTCTCTTTGGCACAAGC
uts2r1_qPCR_R	GGAGATCCAGTAGGTTCTTGCC
uts2r2_qPCR_F	AGTCTGCGTCATCCAGTAATCAG
uts2r2_qPCR_R	AAACCCCAATCTTACCTTCGCA
uts2r3_qPCR_F	CTTTGCCATCGCTCTCAGTTTG
uts2r3_qPCR_R	CAGGCAGGAACACACAACTTTC
uts2r4_qPCR_F	TGCCTTCATCTTGACTCTTCCC
uts2r4_qPCR_R	GTCCACGTTGGGAAACAAATCC
uts2r5_qPCR_F	TTTCTCGTGTGGCTCTTCTCTC
uts2r5_qPCR_R	GCCATTGTGCACGTCTATCTTG
mob4_qPCR_F	AAGAGTGCCCTGCCATTGATTA
mob4_qPCR_R	AGTTTGGCCACAGATGATTCCT
lsm12b_qPCR_F	GAGACTCCTCCTCCTCTAGCAT
lsm12b_qPCR_R	GATTGCATAGGCTTGGGACAAC

sgRNA (CRISPR)	
sgRNA#1	AAAACTGGTGTCAAACGCAATGG
sgRNA#2	TCAAGTGAAGTGCGAGGAGAAGG
cloning of CDS	
urp2_CDS_F	ggatccGTATCTGTAGAATCTGCTTTGCTGC
urp2_CDS_R	tctagaGGCAGAGGGTCAGTCGTGTTAT
Cloning of urp promotor	
URP_prom_F	ggggacaactttgtatagaaaagttgATATTTGATGGCATACATTGTTCCT
URP_prom_R	ggggactgctttttgtacaaacttgTGCACTTGTAAAATGTTGGGTTTCTC

771

Figure 1

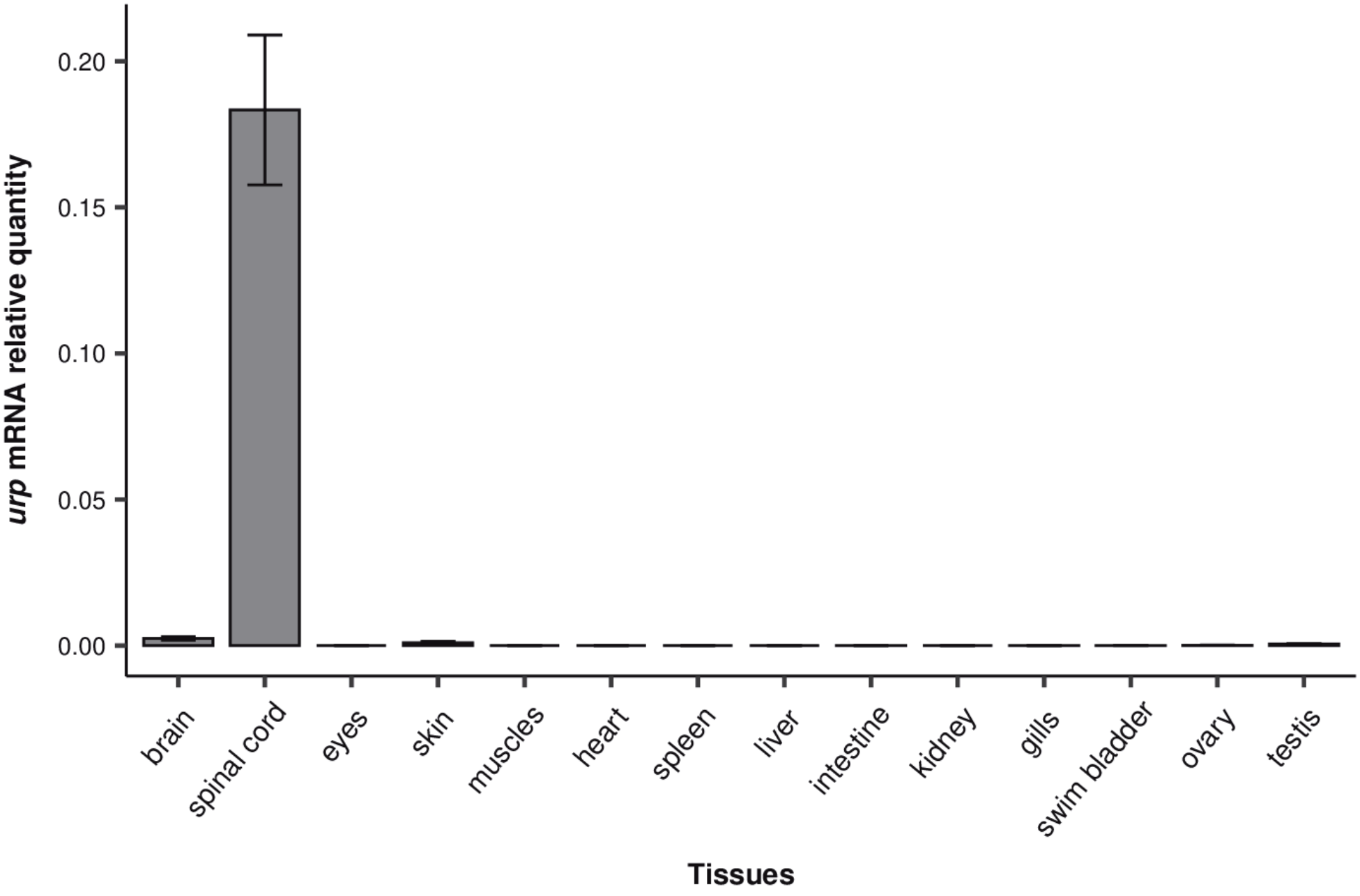
0.20
0.15
0.10
0.05
0.00
urp mRNA relative quantity
brain
spinal cord
eyes
skin
muscles
heart
spleen
liver
intestine
kidney
gills
swim bladder
ovary
testis
Tissues

Figure 2

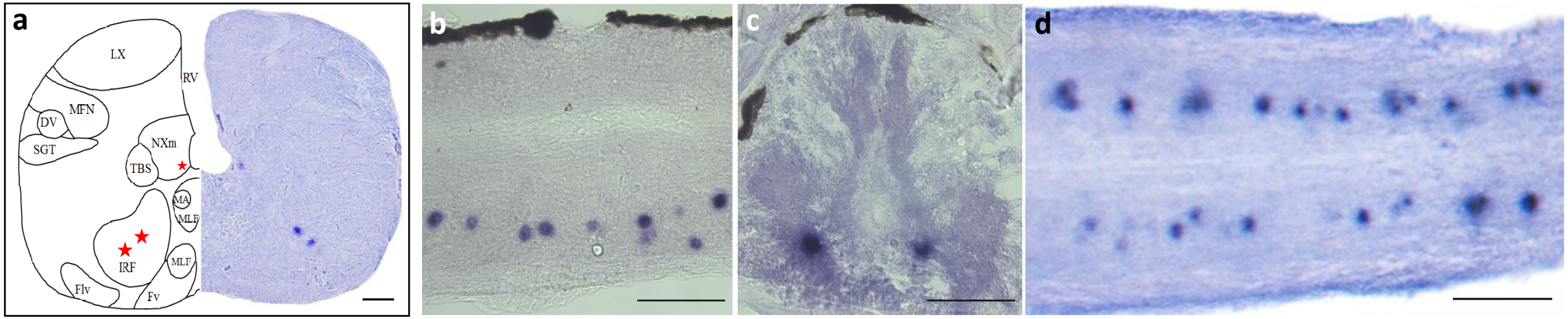

Figure 3

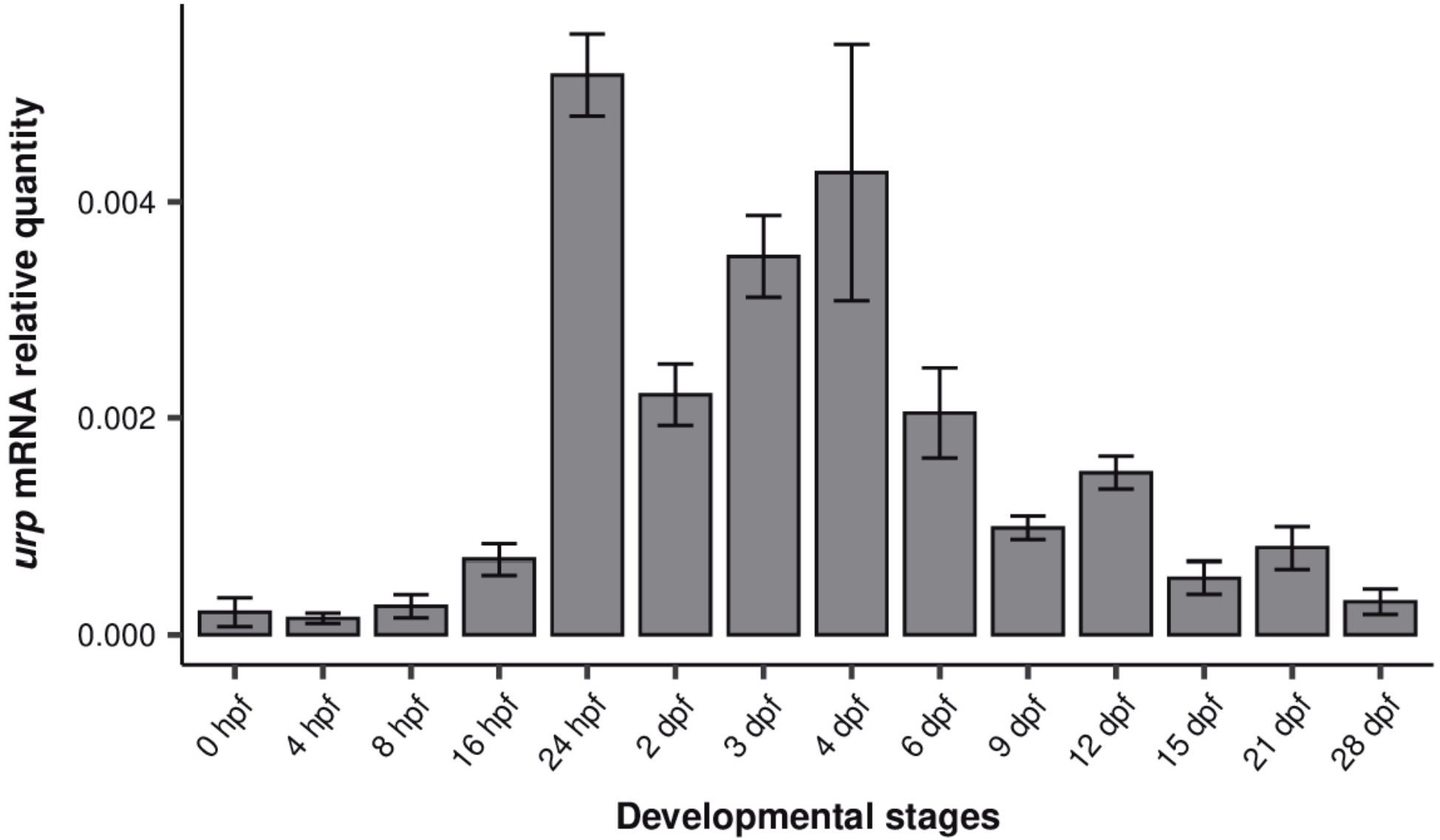
urp mRNA relative quantity
0.004
0.002
0.000
0 hpf
4 hpf
8 hpf
16 hpf
24 hpf
2 dpf
3 dpf
4 dpf
6 dpf
9 dpf
12 dpf
15 dpf
21 dpf
28 dpf
Developmental stages

Figure 4

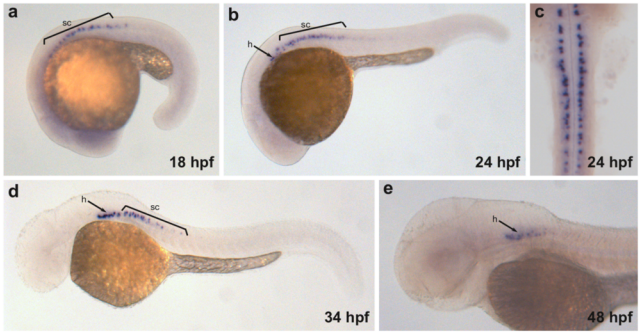

Figure 5

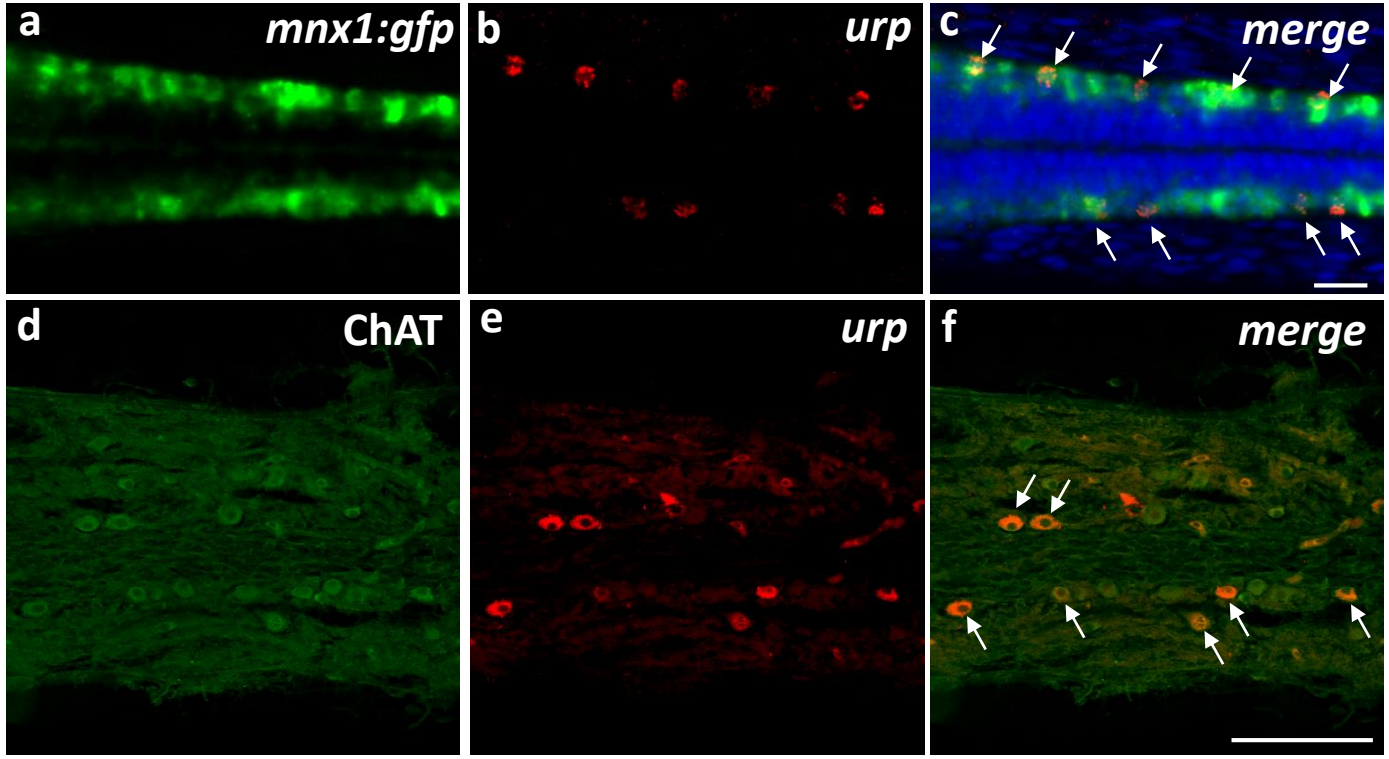

Figure 6

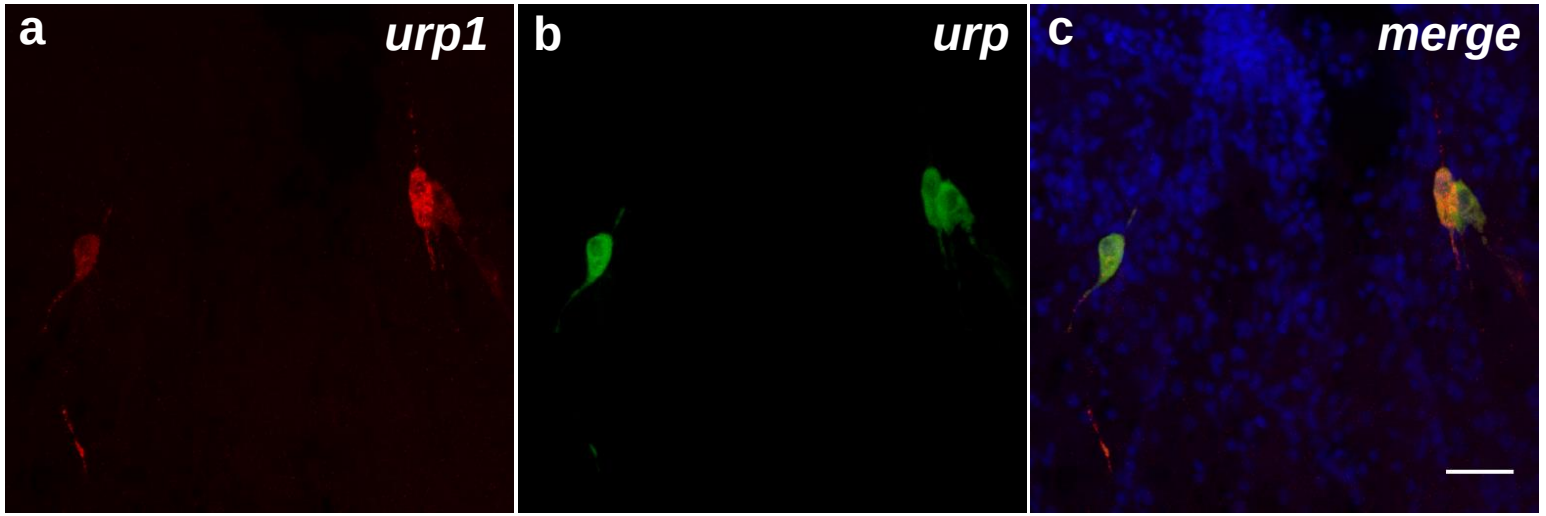

Figure 7

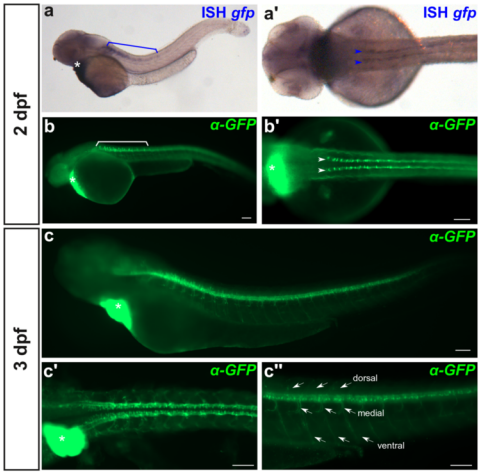
2 dpf
3 dpf
a
ISH gfp
a'
ISH gfp
b
α-GFP
b'
α-GFP
c
α-GFP
c'
α-GFP
c''
α-GFP
dorsal
medial
ventral

Figure 8

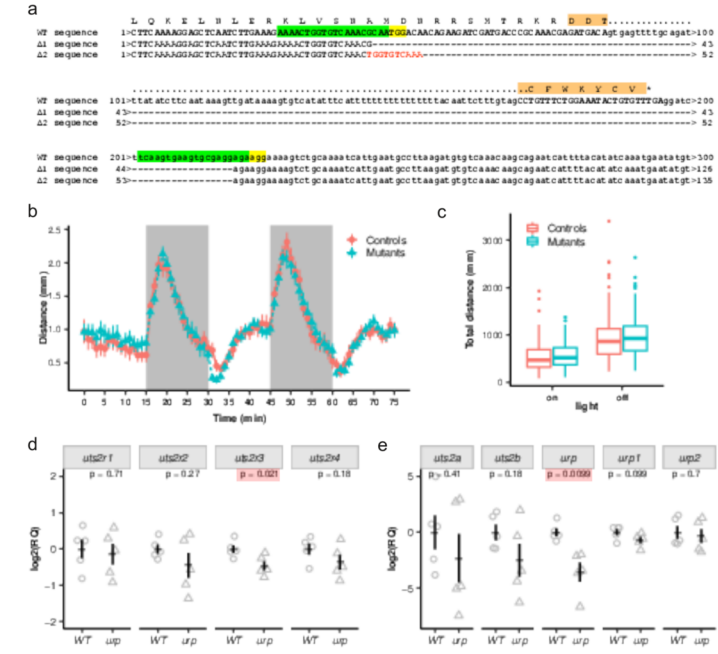
a
b
Distance (mm)
Time (m in)
Controls
Mutants
c
To tal distance (m m)
Controls
Mutants
d
uts2r1
uts2r2
uts2r3
uts2r4
p = 0.71
p = 0.27
p = 0.021
p = 0.18
log2(RQ)
WT
urp
e
uts2a
uts2b
urp
urp1
urp2
p = 0.41
p = 0.18
p = 0.0099
p = 0.099
p = 0.7

Figure 9